






Validation of a 3D numerical model for piled raft systems founded in soft soils undergoing regional subsidence

Andrea J. Alarcón Posse^{1#} , Juan F. Rodríguez Rebolledo¹ , Julián A. Buriticá García¹ ,
Bernardo Caicedo Hormaza² , Edgar Rodríguez-Rincón³ 

Article

Keywords

Numerical analysis
Piled raft
Centrifuge modeling
Hardening soil model
Regional subsidence
Small scale

Abstract

In this paper a 3D numerical model using a software based on the Finite Element Method (FEM), was developed and validated using the results obtained in a geotechnical centrifuge model of a piled raft system founded in soft soils undergoing regional subsidence. The piled raft configuration had nine piles distributed in the center of the raft. The kaolin parameters were obtained, calibrated, and validated for the Hardening Soil Model (HSM), based on laboratory triaxial and oedometer test results. Also, a single pile load test was carried out in the centrifuge to get the resistance parameters used in the FEM. The developed numerical model reproduced satisfactorily soil and foundation consolidation displacements due, not only by the structural service load but also by the pore pressure drawdown. For load distribution on piles and raft, the model reproduces with good agreement the foundation behavior only for the structural service load, for pore pressure drawdown some adjustments on the embedded piles elements shaft and base resistance had to be done. The developed model allowed to identify the most sensitive parameters for this type of simulation, to define the types and stages of analysis that had the best fit for the physical model, and to obtain additional results to those measured in the physical model, e.g., the axial load distribution developed along the piles and therefore the magnitude of the negative skin friction, that is an important load that should be considered for the structural safety review of piled foundations subjected to this complex conditions.

1. Introduction

On many occasions, commercial software based on numerical models are used indiscriminately for the analysis of complex problems without a real understanding of the problem. Also, by ignoring the influence that different geotechnical parameters have on the simulation results. The cases of instrumented structures and/or physical models in laboratory allow obtaining results closer to reality and with a clearer understanding of the phenomenon. However, these results may be limited by the number of case studies, model dimensions, number of variables, time of assembly and execution, type and quantity of instruments and problems related to the installation of the instruments and during monitoring. Regarding the numerical models, they can be calibrated and validated through the results produced by the physical tests and, at the same time, be used to obtain additional results. This calibration and validation process is complex since it must consider the selection of the constitutive model, the adjustment of the parameters, the definition of the initial stress

states and pore pressure, and the definition of the analysis stages. The result of this process allows developing a better understanding of the sensitivity of the different parameters and a more realistic analysis methodology.

In this paper, the case of a piled raft system used on soft soils undergoing regional subsidence was studied. According to Alnuaim et al. (2018), a piled raft is a composite structure with three components: subsoil, raft, and piles. The structural components interact with each other and with the surrounding soil (pile-soil, raft-soil, and pile-raft) to bear vertical, horizontal, and moment loads coming from the superstructure. Luo et al. (2018) refer to this system as an effective foundation due to its efficiency in reducing settlements and improving bearing capacity.

Many papers have been presented to understand the behavior of piled raft systems using different ways of approaching (field test, laboratory test, and numerical modeling). The use of numerical modeling has increased considerably, and it has been used as a tool that allows simulating the behavior of complex structures in real projects. Some models have been

[#]Corresponding author. E-mail address: julianaalarcon2@hotmail.com

¹Universidade de Brasília, Brasília, DF, Brasil.

²Universidad de los Andes, Bogotá, Colombia.

³Universidad Nacional de Colombia, Bogotá, Colombia.

Submitted on July 6, 2020; Final Acceptance on January 20, 2021; Discussion open until May 31, 2021.

DOI: <https://doi.org/10.28927/SR.2021.053620>



This is an Open Access article distributed under the terms of the Creative Commons Attribution License, which permits unrestricted use, distribution, and reproduction in any medium, provided the original work is properly cited.

developed using different software and constitutive models mainly to evaluate how the pile spacing, load sharing, pile length, and diameter affect the settlement of the foundation (Cui et al., 2010b; Lee et al., 2010; El-Mossallamy, 2008; Roy & Chattopadhyay, 2011; Cho et al., 2012; van Tran et al., 2012b; Rodríguez-Rebolledo et al., 2015; Watcharasawe et al., 2015; Banerjee et al., 2016; Sinha & Hanna, 2017; Zhang & Liu, 2017; Alnuaim et al., 2017; Khanmohammadi & Fakharian, 2018; Luo et al., 2018; Mali & Singh, 2018). Although some of those works consider consolidation analyses, few studies have really focus on simulating the subsidence process in a more precise way using more accurate constitutive models that represent the soil behavior, which can lead to a closer analysis of the system's behavior.

Geotechnical centrifuge modeling is an advanced physical modeling technique that provides data for investigating mechanisms of deformation and failure and for validating analytical and numerical methods (Ng, 2014). Some authors have presented centrifuge tests that evaluate the influence of regional subsidence in a different type of constructions (Sun et al., 2008; Cui et al., 2010a; Cheng et al., 2011; Tang et al., 2012; Wang et al., 2013; Zhang et al., 2017a, b). On the other hand, various researches have been done using piled raft system on centrifuge like Thaher & Jessberger (1991), Horikoshi & Randolph (1996), Bajad & Sahu (2008), Goh & Zhang (2017), among others. van Tran et al. (2012a), Rodríguez-Rincón (2016) and Rodríguez-Rincón et al. (2020), focused specifically on the behavior of the piled raft under the effects of regional subsidence, assessing not only settlements but also load distribution.

The aim of this work is to develop and validate a three dimensional (3D) numerical model based on the Finite Element Method (FEM, Plaxis 3D) capable of simulating the complex behavior of a piled raft system founded in soft soils undergoing regional subsidence. For this purpose, the results obtained by Rodríguez-Rincón (2016) of a geotechnical centrifuge model were used. This model allows to identify the most sensitive parameters for this type of simulation, to define the types and stages of analysis that had the best fit to the physical model, and to obtain additional results to those measured in the physical model, e.g., the axial load distribution developed along the piles and therefore the

magnitude of positive and negative skin fractions and point load. According to Auvinet & Rodríguez-Rebolledo (2017), the effect of the negative skin friction developed on piles shafts should be considered for the structural safety review and for the estimation of the long-term displacements of piled foundations.

Being one of the most complete constitutive models of Plaxis, the Hardening Soil Model (HSM) was chosen to simulate the soil behavior. To complete the data needed for the numerical simulation, new laboratory tests, and a load test in a single pile in the centrifuge were performed. The parameters obtained for the HSM were calibrated through numerical modeling of the tests using the *SoilTest* module of Plaxis software. Based on the evaluation and calibration of these parameters, a geotechnical model profile to represent the centrifuge experimental test is proposed. The calibration by displacements and by loads distribution of the 3D numerical model by comparison with the centrifuge test results is presented and discussed. Finally, the axial loads developed along the center, border and corner piles, for the different stages of the problem, are presented and interpreted.

2. Materials and methods

2.1 Case study - centrifuge model

The case study is based on a centrifuge model developed by Rodríguez-Rincón (2016); Rodríguez-Rincón et al. (2020) at the Geotechnical Models Laboratory of the Universidad de Los Andes, Bogota, Colombia. The model is focused on the evaluation of the behavior of piled raft systems in soft soils along the consolidation process generated both by the structural load and by the pore-pressures drawdown. The decrease of the pore pressure value was associated with the subsidence process induced by the extraction of water from deep permeable layers (Figure 1).

The soil profile used was composed of three layers of a mixture of kaolin with water content at 1.5 times the liquid limit, divided by two sand layers that work as a filter and a bottom layer as drainage. This profile is intended to represent a soft clay soil typical of the city of Bogotá. To physically model a piled raft foundation, a 70 g centrifugal acceleration was adopted due to the capacity of the modeling box (boundary conditions), the size of elements sections after scaled and

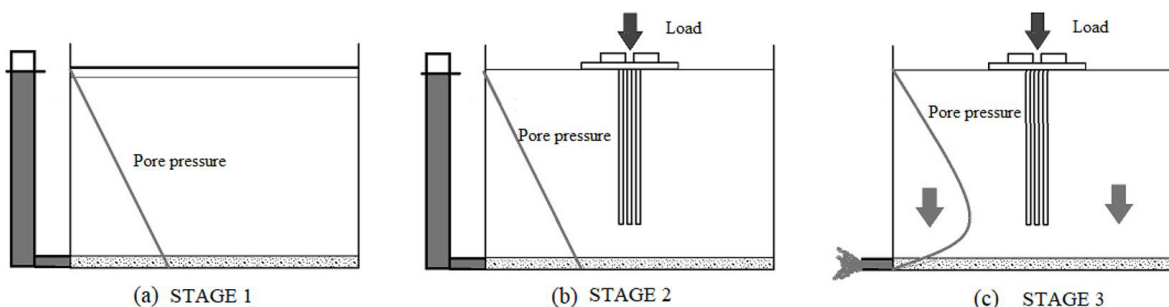


Figure 1. Representation of pore pressure conditions at testing stages. Adapted from Rodríguez-Rincón (2016).

the size and capacity of the available instrumentation. The configuration of the piled raft is a model with nine piles distributed in the center of the raft, with a pile spacing of two diameters. Table 1 summarizes the dimensions and parameters of the piled raft elements.

The test setup that was employed to evaluate the performance of the piled raft is shown in Figure 2. The instrumentation used were composed of three linear variable differential transducers (LVDT) on the soil and three on the raft, four piezometers and a load cell. Four piles were also instrumented with miniature load cells to measure the load transmitted to the top piles. Important results were obtained regarding the piled raft behavior and were used for the present paper.

2.2 Hardening Soil Model (HSM)

The research was conducted by using Plaxis 3D software, which is widely used for geotechnical analysis. As mentioned by Rodríguez-Rebolledo et al. (2019), soil constitutive models have advanced significantly from basic models that idealize the soil as a linear elastic medium or

Table 1. Elements dimensions of the piled raft for models with a scale factor of 70g.

Element	Parameter	Model
Raft	Material	Aluminum
	Thickness	13 mm
	Young's modulus	70000 MPa
	Width	200 mm
	Length	200 mm
Piles	Material	Aluminum
	Diameter	9 mm
	Young's modulus	70000 MPa
	Length	320 mm

a perfectly plastic linear elastic medium. The HSM is an isotropic hardening double surface plasticity model that gives more accurate displacements patterns for conditions at working load (Schanz et al., 1999). This model considers both theories of the non-linear elasticity and the plasticity, representing a significant advance in comparison with the basic linear elastic models (LE) and the elastic-perfectly plastic model of Mohr-Coulomb (MC). This model is available in the Plaxis software and was implemented by the program initially as an extension of the MC model (Nordal, 1999). Although the results obtained with this model are closer to “reality”, it requires a greater number of input parameters that demand more experimental tests. The HSM basic characteristics are given by:

- Total strains are calculated using a stress-dependent stiffness according to a power law (input parameter m);
- Shear hardening: plastic straining is due to primary deviatoric loading (input parameter E_{50}^{ref});
- Compression hardening: plastic straining is due to primary compression (input parameter E_{oed}^{ref});
- Failure according to MC criterion (input parameters c' and ϕ);
- Stiffness defined by loading and unloading/reloading conditions (input parameters E_{ur}^{ref} and v_{ur});
- Non-associated flow rule assumed for shear hardening (input parameter ψ);
- Associated flow rule assumed for compression hardening.

2.3 Parameters determination from laboratory tests

With the aim of numerically reproduce the behavior of a pile raft foundation system and to take into account the need to determine the mechanical parameters of the HSM,

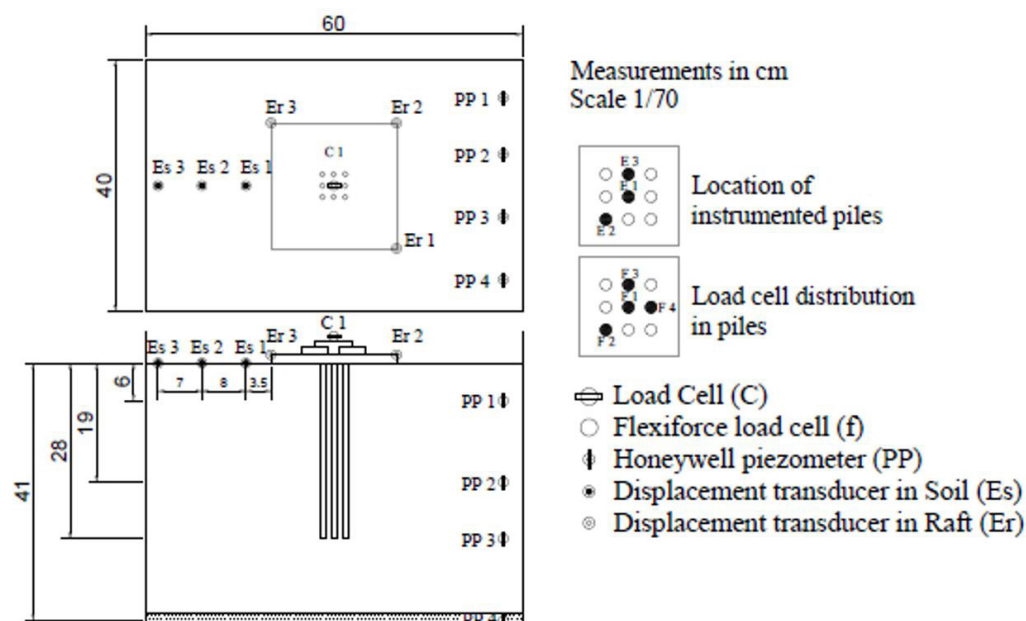


Figure 2. Distribution of the instrumentation on the centrifuge model M3. Adapted after Rodríguez-Rincón (2016).

it was necessary to carry out tests on a kaolin soil mixture whose profile represented the one proposed by Rodríguez-Rincón (2016). In this way, it was possible to experimentally determine the behavior of the soil in a different stress state, as well as the value of the axial pile resistance. The procedure described by Rodríguez-Rincón et al. (2020) was used for the fabrication of the soil mixture in the experiments. The results of the oedometer, triaxial tests, and the pile load test in the centrifuge are presented next.

a) Oedometer tests data

The oedometer tests were conducted on three samples at different layers of the fabricated soil labeled M1, M2 and M3. Table 2 shows the calculated values of the reference oedometer modulus (E_{oed}^{ref} , $E_{ur,oed}^{ref}$) and the parameter that defines the dependency level of the strains on the stress state (m). The methodology to calculate the parameters was the one suggested by Surarak et al. (2012) and Rodríguez-Rebolledo et al. (2019). The results are plotted in Figure 3.

b) Triaxial tests data

Three isotropically drained consolidated triaxial tests (CID) were conducted at the three distinct layers of the experiment M1 to M3. The confining pressures σ_3 used for the M1 and M2 samples were 100, 200, 300 kPa, and for the M3, σ_3 was equal to 200, 300, and 500 kPa. The friction angle (ϕ') obtained were 25°, 22°, and 18°; whereas the cohesion (c') was 21, 40 and 1 kPa, respectively. The reference modulus at 50% of strength (E_{50}^{ref}) and power m determined from the CID tests using double log scale plots are given in Figure 4. These values are summarized in Table 3 and were also obtained following the methodology described by Surarak et al. (2012) and Rodríguez-Rebolledo et al. (2019).

2.4 Calibration of parameters

To calibrate the soil parameters listed in Tables 2 and 3, the CID triaxial and oedometer tests were modeled in Plaxis using the *SoilTest* tool. This tool is a quick and convenient procedure to simulate basic soil lab tests based on a single point algorithm, i.e., without the need to create a complete finite element model (Brinkgreve et al., 2018). It works with the inputted soil parameters obtained from a site investigation to compare with the behavior as defined by the soil model chosen (HSM in this case).

In order to obtain suitable parameters to give the best fit results, the input parameters were adjusted, as presented in Figures 5, 6 and 7, for layers M1, M2 and M3, respectively. The results from the three layers reveal good agreements among all the stress-strain and stress path behavior for different confining pressure values ($\sigma_3 = 100, 200, \text{ and } 300 \text{ kPa}$). Although the M3 layer results (Figure 7) calculated were not as successful as those of the M1 (Figure 5) and

Table 2. Parameters calculated from oedometer tests.

Layer	E_{ur}^{ref} (kPa)	m	E_{oed}^{ref} (kPa)	m
M1	4,976	1.13	830	0.99
M2	6,164	1.08	1,347	0.82
M3	7,707	0.91	2,214	0.5

Table 3. Parameters calculated from triaxial tests.

Layer	E_{50}^{ref} (kPa)	m	ϕ' (°)	c' (kPa)
M1	1,413	0.8	25	21
M2	2,044	0.5	22	40
M3	843	1	18	1

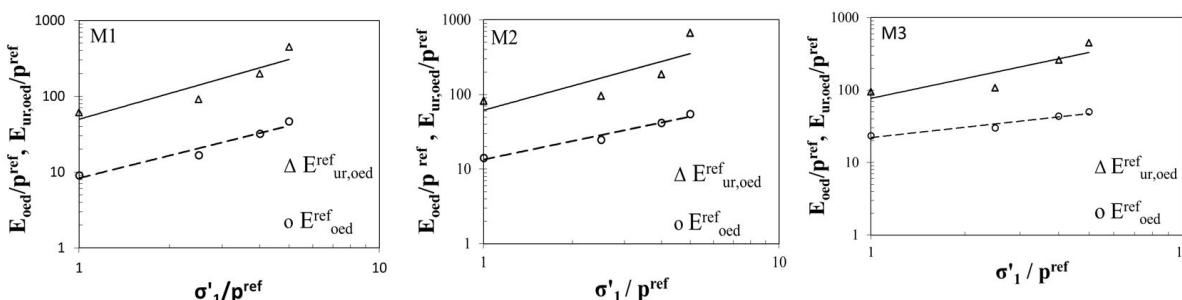


Figure 3. Oedometer Modulus versus consolidation pressure calculated from one-dimensional consolidation tests.

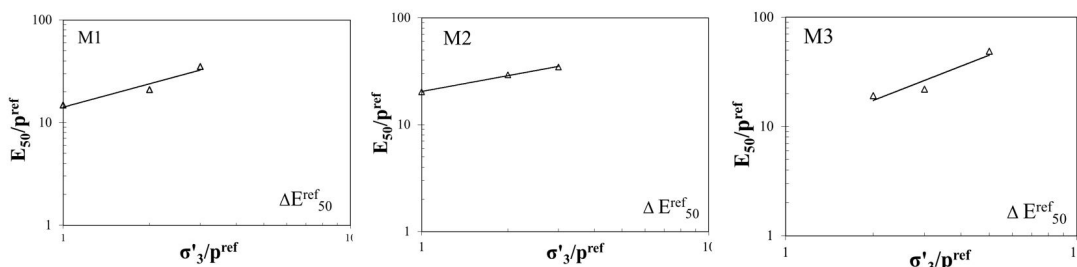


Figure 4. Variation in E_{50} with confining pressure.

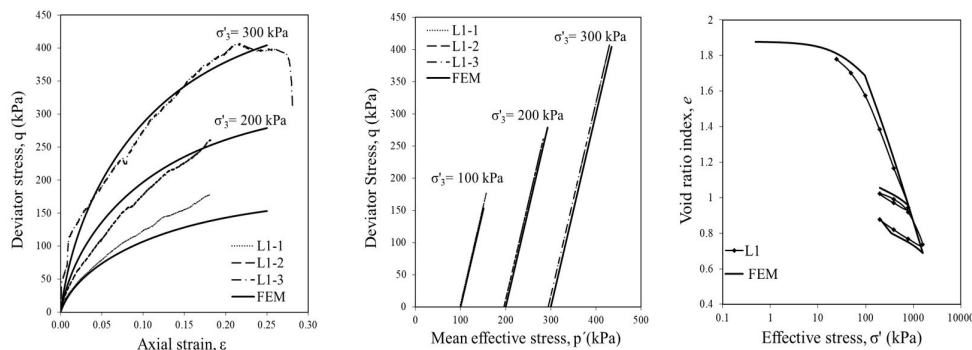


Figure 5. CID triaxial and oedometer test results and their FEM simulations with HSM for layer M1.

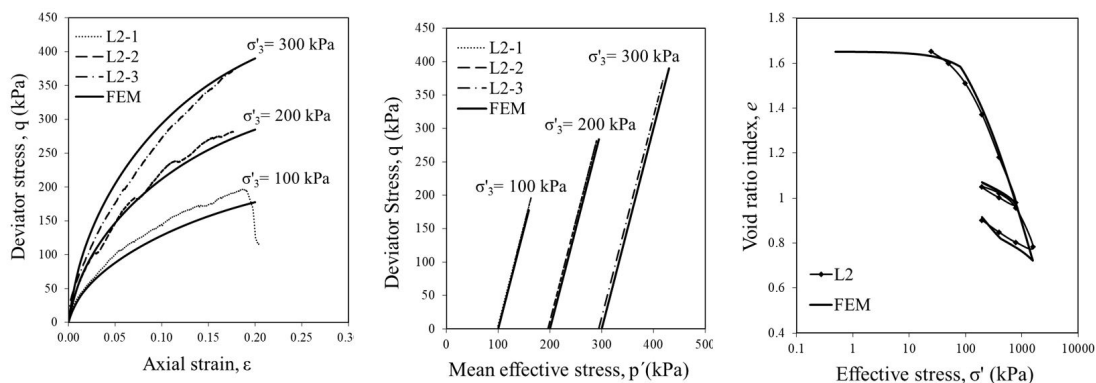


Figure 6. CID triaxial and oedometer test results and their FEM simulations with HSM for layer M2.

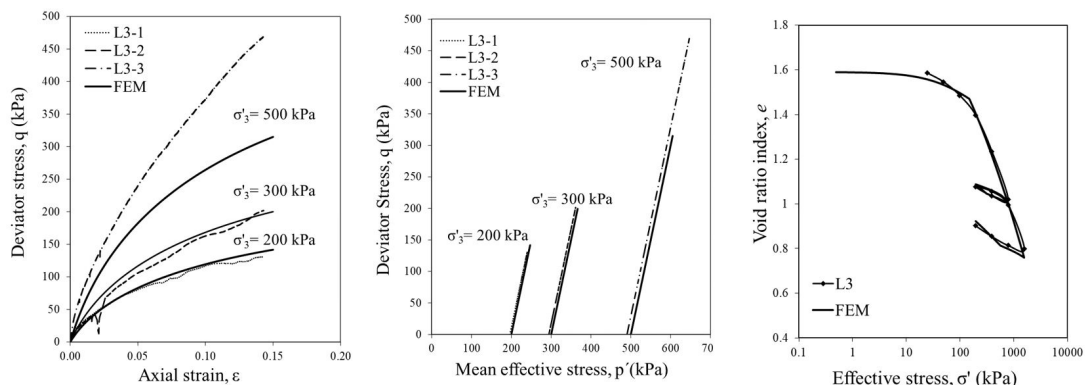


Figure 7. CID triaxial and oedometer test results and their FEM simulations with HSM for layer M3.

M2 (Figure 6) layer, since they were underestimated for the confining pressure of 500 kPa, nevertheless, it can be stated that the HSM predictions agree reasonably well with the triaxial test results.

As the stress state has a significant variation throughout the depth, for the numerical simulation, the soil profile was divided into several layers using the over consolidation ratio (OCR) values as a criterion. Besides being an indicator of the stress state, the OCR is one of the input parameters of the HSM. Also, the ground-water table was considered at 3.5m of depth as originally proposed by Rodríguez-Rincón (2016). Since in the process of fabrication and lowering of the water level a stiff layer was formed on the surface, the

parameters adopted for this layer were the ones calibrated for a stiff clay by Surarak et al. (2012). The geotechnical parameters for the different soil layers obtained for the numerical simulations are presented in Table 4.

2.5 Long term bearing capacity estimation

Having the load measured on the top of the piles from the centrifuge, it was considered fundamental to calibrate the model not only with the displacements but also with the load distribution, so to have a more accurate model. In consequence, a pile load test on an isolated pile was carried out in the centrifuge to better establish the long-term parameters for the numerical model.

Table 4. Geotechnical parameters for the soil profile.

Layer	z m	γ kN/m ³	σ'_0 kPa	σ kPa	σ_p kPa	c' kPa	ϕ °	k_0	k_0^{nc}	E_{50}^{ref}	E_{ur}^{ref}	E_{oed}^{ref}	m	ν	k m/h	OCR	
										MPa	MPa	MPa					
M1	L-1	0 - 3.5	18.67	10	28	170	11.5	28	1.24	0.53	9.5	30	12	1	0.2	8×10^{-6}	6.07
	L-2	3.5 - 6	16.68	30	75	170	21	25	1.2	0.58	1.41	10	1	1	0.2	8×10^{-6}	5.66
	L-3	6 - 9	16.68	50	125	191	21	25	0.97	0.58	1.41	10	1	1	0.2	8×10^{-6}	3.39
M2	L-4	9 - 19	17.03	81	200	223	20	22	0.92	0.62	2.4	15	1.55	1	0.2	8×10^{-6}	2.77
M3	L-5	19-23	17.03	141	342	342	20	17	0.74	0.71	2.5	16	1.58	0.8	0.2	8×10^{-6}	1.27
	L-6	23-28	17.03	176	425	382	20	17	0.69	0.71	2.5	16	1.58	0.8	0.2	8×10^{-6}	1.01

L-1: Crust, over consolidated high plasticity clay subject to wetting and drying cycles; L-2 to L-6: Soft clay formation, from over to normally consolidated high plasticity saturated clay.

Table 5. Parameters of the pile.

Parameter	Value	Unit
Axial skin resistance	11.38	kN/m
Base resistance	205	kN

The test was performed in a cylindrical container with an inner diameter of 30 cm and 60 cm in height, and a model scale of 1/70 was used with a centrifugal acceleration of 70g. The instrumented pile was made of an aluminum bar with a 6 mm diameter and Young’s modulus of 70 GPa. The outer diameter of this pile was 10 mm with 400 mm of length. The applied axial load was monitored by a central load cell, and four extra lateral units were used to measure the axial load transfer along the pile shaft during the tests. Also, a linear variable differential transducer (LVDT) was employed to track the pile displacement during test (Figure 8).

The installation of the model pile was carried out at lg with a compression rate of about 0.5 mm/s. This model was tested in two stages: first, without loading the pile till stabilization of the readings so to guarantee the adherence of the pile shaft with the soil; and second, with the subsequent development of the load test. In general, each load increment was held until the cells had reached their steady state condition before another load increment was further applied. After stopping the centrifuge, vane tests were conducted at different depths to check on the undrained shear strength.

The load and displacement data are shown in Figure 9. Test results are expressed in the prototype scale unless stated otherwise. The maximum applied load was 539 kN. Table 5 presents the input parameters that were needed for the model, in terms of pile shaft and base resistance for long term behavior. It was observed that the pile-soil adherence

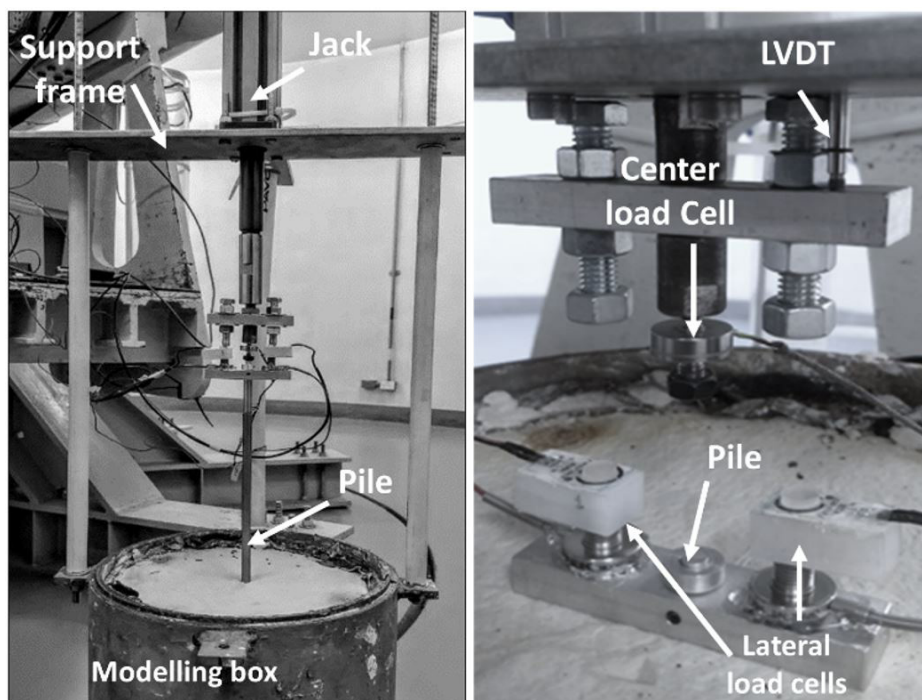


Figure 8. Centrifuge model assembly and instrumentation.

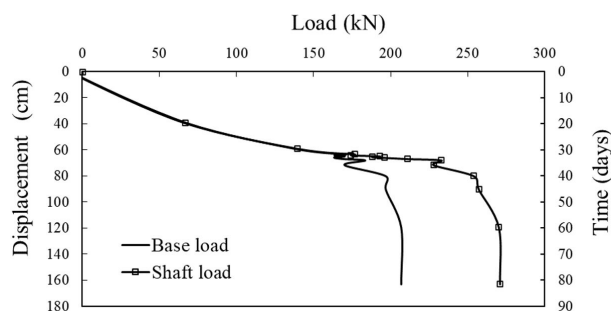


Figure 9. Displacement and time versus load curves.

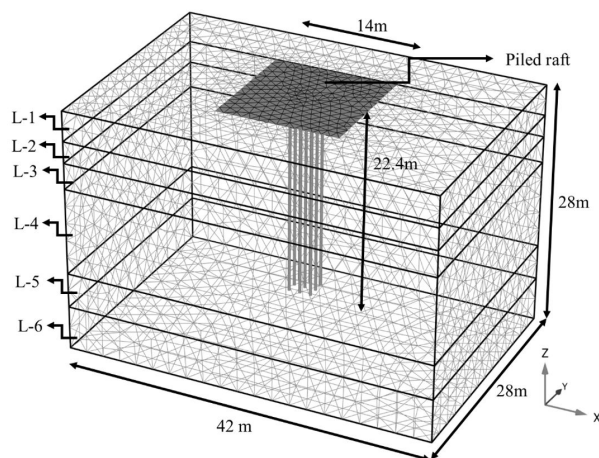


Figure 10. Geometry and mesh of the proposed 3D FEM model.

Table 6. Parameters of the structural elements

Element	Parameter	Value
Plate (Raft)	Unit weight	25 kN/m ³
	Thickness	1.147 m
	Young's modulus	35 GPa
	Width	14 m
	Length	14 m
	Unit weight	25 kN/m ³
Embedded beams (Piles)	Diameter	0.63 m
	Young's modulus	30 GPa
	Length	22.4 m
	Axial skin resistance	11.38 kN/m
	Base resistance	205 kN

is low, which has consequently generated a significant displacement of the pile.

2.6 Proposed model

To model the structural components, such as concrete piles and raft, a linear elastic constitutive model was assumed. Regarding the element type used for the design of the piled raft foundation, a plate element for the raft and embedded beams for the piles, were assumed. Plates are structural objects used to model structures in the ground with a significant flexural rigidity that does not allow plastification, only linear elastic behavior. As for an

embedded beam element, it is defined as a structural object with special interface elements providing the interaction between the beam and the surrounding soil. The interaction involves a skin friction as well as a base resistance, which is determined by the relative displacement between soil and pile. This element type was chosen instead of the volume elements since with them it is possible to generate a mesh with fewer finite elements, thus decreasing the analysis time (Oliveira, 2018).

The geometry of the piled raft and the boundary conditions of the soil body are presented in Figure 10. Their properties are listed in Table 6. The horizontal movements in the four boundaries were fixed as well as the vertical displacement at the lower frontier. Regarding the water boundary conditions, it shall be noticed that the water flow exit was restricted in the lower edge in all phases before pore pressure drawdown.

2.7 Stages of analysis

A graphic representation of the stages of the centrifuge test performed and the conditions of each of them are presented in Figure 11, where time intervals are also specified. The numerical model was analyzed in terms of effective stresses, with drained parameters and initial drained conditions. According to Rodríguez-Rebolledo (2011), this type of analysis is applied to obtain stresses, strains, and displacements before, during, and after the consolidation process, which is the purpose in the present work.

To represent the centrifuge test, the considered calculation phases are described below:

- *Initial Phase*: at this stage, the initial stress of the soil is generated. This stress state is usually characterized by an initial vertical effective stress. In Plaxis, initial stresses may be generated by using the K_0 procedure that is a special calculation method to define these stresses, considering the loading history of the soil (Brinkgreve et al., 2018) (Plaxis, 2018);
- *Phase 1, construction and loading*: in this phase it was simulated the construction of the piled raft and the application of the load along the foundation surface, in accordance with the experimental test. A consolidation calculation was used to analyze the development of pore pressure as a function of time. As it is possible to apply load in this analysis, a value of 38.25 kPa was applied in 5000 hours corresponding to the interval time from t_c - t_E of the centrifuge test, Figure 11;
- *Phase 2, consolidation*: in this phase, the same analysis was used as in the previous one to represent the interval time from t_E - t_F (Figure 11) in which the load has reached its maximum value. The load was maintained for more 8,914 hours;
- *Phases 3 to 6, pore water pressure drawdown*: these phases correspond to the Stage 3 previously explained in Figure 11 in which a drawdown of pore pressure

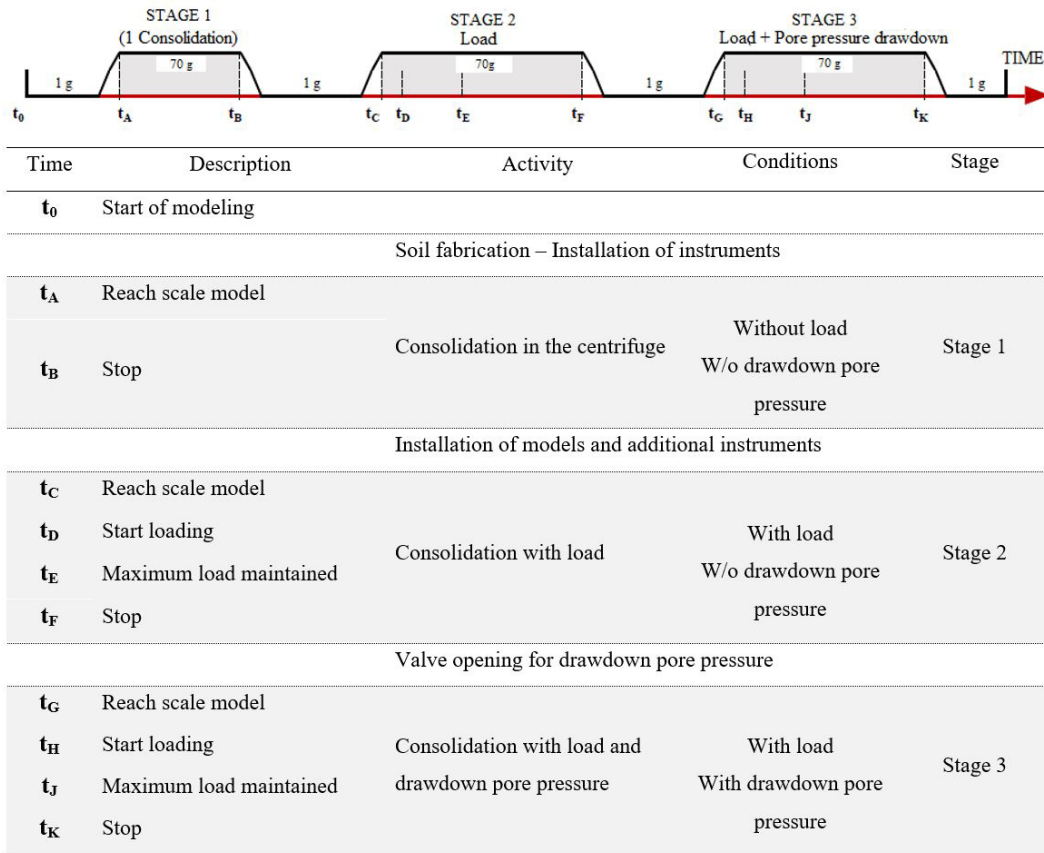


Figure 11. Description of the test carried out in the centrifuge and the pore pressure condition in the three stages. Adapted from Rodríguez-Rincón (2016).

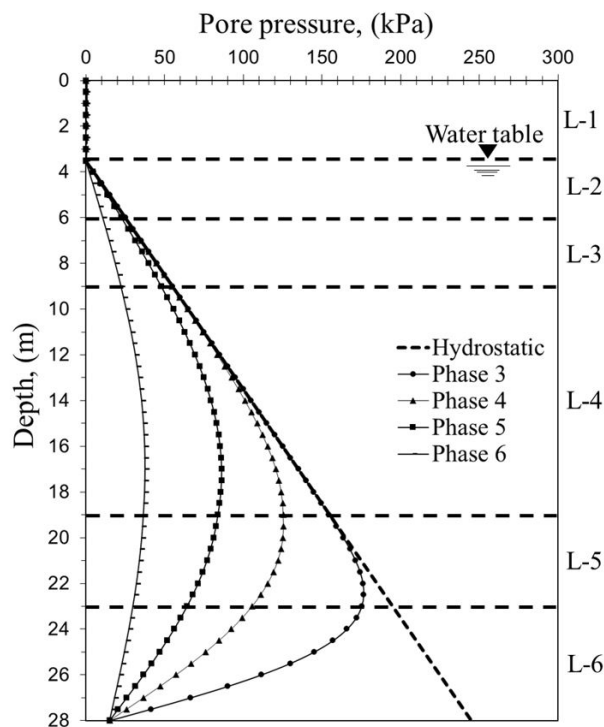


Figure 12. Pore water pressure conditions.

Table 7. Description of the phases that simulated the drawdown pore pressure.

Phase	Consolidation degree (%)	Time (hr)
3	20	606,8
4	40	1736
5	60	2868
6	88	7787

is generated, Figure 12. Table 7 summarizes each of these phases, that correspond to a particular degree of consolidation to be reached in a certain period.

In the last stage of the centrifuge test, drawdown phase, the soil was brought to an 88% degree of consolidation. This stage was divided in four parts in the numerical model, where pore pressures were sequentially imposed to reach 20, 40, 60 and 88% of degree of consolidation. The piezometer data obtained in the centrifuge test was measured very close to the filter layers, so it could not be used as an initial input in the numerical simulation to model the exact decrease of pore pressure. Consequently, the isochrones presented in Figure 12 were established by using the finite difference method.

3 Results and discussions

3.1 Calibration by displacements

The displacement-time curve for the piled raft foundation, under vertical loading and pore pressure drawdown, obtained from the centrifuge test is presented along with the results obtained from FEM. Figure 13 shows the displacements measured at a point over the soil near the raft (*Es1*) with respect to time. In the first stage of the test, the results in the prototype are reasonably close to those from the centrifuge. Regarding the drawdown pore pressure phase, the results move away slightly, although the tendency is similar.

The displacements on the foundation system in the model were measured in three corners on top of the raft, labeled as *Er₁*, *Er₂* and *Er₃*. The results are plotted in Figure 14. The experimental centrifuged results measured in the three corners of the raft were slightly different, and this can be due to a possible uneven load application, that probably caused an unequal load distribution among the system's components. When comparing the model and FEM results, it is observed that the two paths are reasonably close. Hence, with close results presented for soil and foundation, and a quite accurate representation of the phenomenon, therefore is possible to consider that the numerical model is calibrated by displacements for the centrifuge tests carried out in the laboratory.

FEM displacement results obtained from phase 2 (consolidation with load) and the final phase 6 (consolidation with load and decrease of pore pressure) are presented in Figures 15 and 16, respectively. The subsidence due to drawdown can be seen in Figure 16, where the settlements were considerably larger than in the previous phase (Figure 15). In phase 2 the maximum settlements reached up to 6 cm in the raft region, and plastification points are observed at the tip of the piles. At the end of phase 6 the maximum settlement was approximately 50 cm, which is 8 times the one obtained in phase 2. These comparative results do evidence

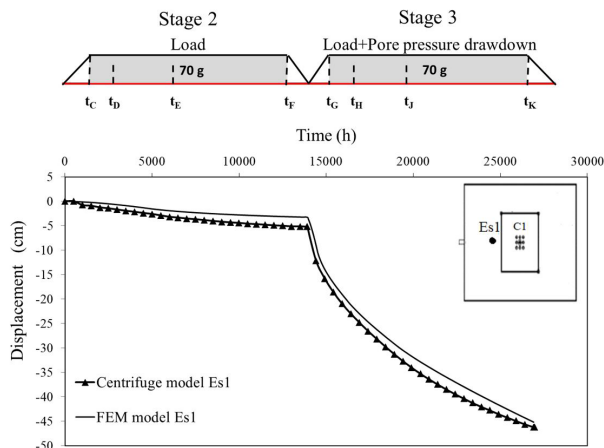


Figure 13. Displacements *versus* time curves obtained at point *Es1* by centrifuge and FEM models.

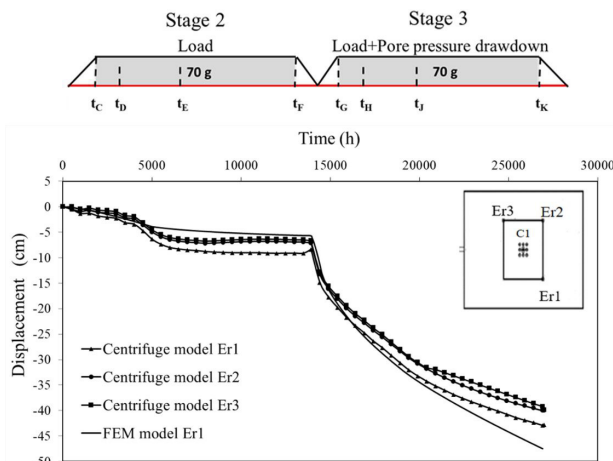


Figure 14. Displacements *versus* time curves obtained at raft corner points *Er1*, *Er2* and *Er3* by centrifuge and FEM models.

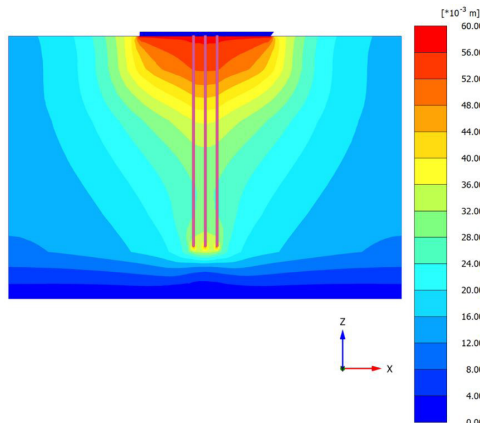


Figure 15. Vertical section at the center of the FEM model showing the total vertical displacements obtained at the end of Phase 2.

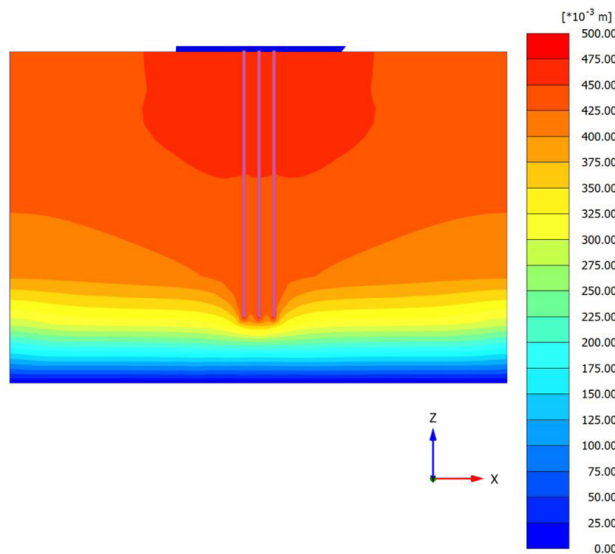
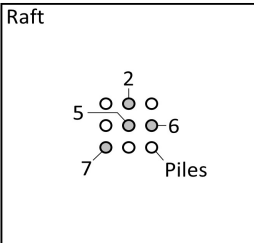


Figure 16. Vertical section at the center of the FEM model showing the total vertical displacements obtained at the end of Phase 6.

Table 8. Comparison between the centrifuge and FEM load values measured at the top of the piles for each stage of the test.

Raft	Element	Stage 2			Stage 3		
		Load		Dif. %	Load		Dif. %
		Centrifuge	FEM		Centrifuge	FEM	
	Pile 2	196 kN	226 kN	+15	347 kN	156 kN	-122
	Pile 5	173 kN	228 kN	+32	393 kN	222 kN	-77
	Pile 6	164 kN	227 kN	+38	463 kN	172 kN	-169
	Pile 7	215 kN	241 kN	+12	352 kN	158 kN	-122
	All piles	1,753 kN	2,098 kN	+20	3,421 kN	707 kN	-384
		13%	16%	+23	26%	5%	-420
Raft		87%	84%	-3	74%	95%	+28

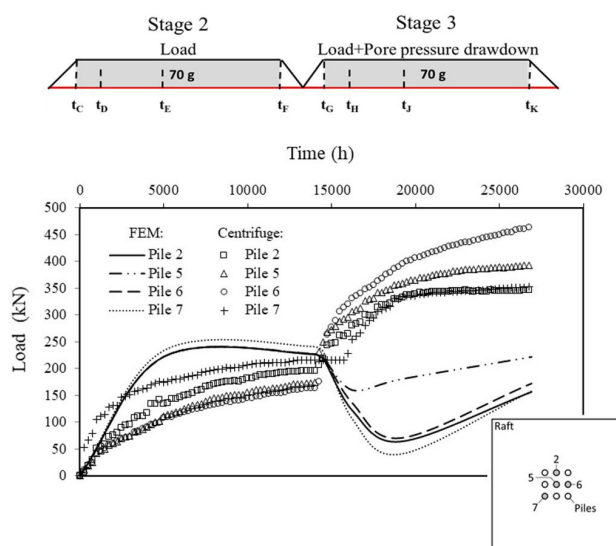


Figure 17. Load versus time curves obtained at the top of the instrumented piles 2, 5, 6 and 7 by centrifuge and FEM models.

the distinct phenomena and resulting engineering behavior that take place on a typical system founded in this type of environment, where loading and subsequent drawdown of pore water pressure can happen.

3.2 Calibration by load distribution

The load-time curves for each instrumented pile, under vertical loading and pore pressure drawdown, obtained from the centrifuge test are presented along with the results obtained from FEM. Figure 17 shows the load measure at the top of piles 2, 5, 6 and 7 with respect to time. In the first stage of the test, the results in the prototype are reasonably close to those from the centrifuge. Regarding the drawdown pore pressure phase, the values obtained with the FEM are considerably lower than those obtained experimentally. Table 8 shows a comparison of the results obtained with both models at the end of each stage. For stage 2 differences between FEM and centrifuge models from 12 to 38% were obtained, while for stage 3 from -77 to -169%. Centrifuge model shows that from stage 2 to 3 load transmitted by piles increases (from 13% to 26%) while load transmitted by raft decreases (from

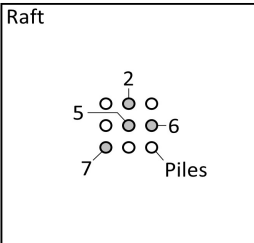
87 to 74%). As explained by Rodríguez-Rincón et al. (2018) this is because, in stage 3, when pore pressure drawdown occurs, the soil continues to settle, a movement that is not accompanied by the raft, generating an apparent emersion process, and hence, a reduction of contact between the soil and the raft. This phenomenon is not developing in the FEM model because the considered skin resistance of the piles is not enough to allow the generation of the negative skin friction necessary for this.

The pore pressure drawdown generated in stage 3 produces an increment in effective stresses throughout the compressible soil, leading to an increase in shear resistance. The FEM results show that the embedded pile element does not consider the increase of the shear resistance parameters related to skin friction that happen when the soil is subjected to a consolidation process. To overcome this problem, the input parameters for this element, in stage 3, were further adjusted to properly “match” the centrifuge data in a sort of back-analysis. This analysis was made running the model increasing the base and axial skin resistance gradually until satisfactory match the data measured.

Figure 18 shows the load measure at the top of piles 2, 5, 6 and 7 with respect to time after adjustment of base and skin resistance of embedded piles elements. It is possible to observe a behavior more like that of the experimental model, mainly in the magnitude of the load obtained at the end of the stage. The differences between models during pore pressure drawdown are mainly due to the type of drainage considered in each one. In the model of the centrifuge this is developed in a more “efficient” way because it occurs through three draining layers, obtaining a stabilization of most of the loads for a time of approximately 20,000 hours. For the numerical model, the drainage was simulated in a more “realistic” way considering only a draining layer down to the compressible stratum, observing its stabilization only until the end of the consolidation process.

Table 9 shows a comparison of the results obtained with both models at the end of each stage, after being adjusted. It is possible to observe that now, for stage 3, the numerical model is simulating the same behavior as the experimental one, presenting variations in the piles loads from -4 to 21%.

Table 9. Comparison between the centrifuge and FEM load values measured at the top of the piles for stage 3, after adjustment.

Raft	Element	Stage 2			Stage 3		
		Load		Dif. %	Load		Dif. %
		Centrifuge	FEM		Centrifuge	FEM	
	Pile 2	196 kN	226 kN	+15	347 kN	382 kN	+10
	Pile 5	173 kN	228 kN	+32	393 kN	477 kN	+21
	Pile 6	164 kN	227 kN	+38	463 kN	430 kN	-7
	Pile 7	215 kN	241 kN	+12	352 kN	298 kN	-15
	All piles	1,753 kN	2,098 kN	+20	3,421 kN	3,293 kN	-4
		13%	16%	+23	26%	25%	-4
Raft		87%	84%	-3	74%	76%	+3

This was only possible by increasing the base and axial skin resistance of the embedded piles elements, during stage 3, in about 3.5 times, this research demonstrates the limitation in the use of this type of elements for the simulation of this kind of problems. To avoid this problem, two solutions are proposed:

- 1) determine the long-term base and skin resistance of the embedded piles using previously a simple 2D FEM model (axisymmetric), through the simulation of a load test of a single pile in a medium previously subjected to pore pressures drawdown.
- 2) use of volume elements for problems with a relatively small number of piles, the use of this type of elements can lead to exceptionally large finite element meshes and therefore high or even irrational computational costs (time and memory).

3.3 Obtaining the axial load along the pile

Having the model calibrated, it was possible to obtain the variation of axial loads with depth for center, border and corner piles (Figure 19), which allows to properly access the negative skin friction that can be eventually generated.

For phase 2 (Figure 19a), due to the high rigidity of the raft and to the proximity between piles, the load transmitted to the three elements is practically the same, slightly higher (+13 kN) for the corner one. For phase 6 (pore pressure drawdown) the model evidences the development of negative skin friction in the three piles (Figure 19b), being higher in the corner and lower in the center one. As excess pore pressure dissipates, the neutral level of the piles stabilizes at a depth between 15 to 16 m. These results agree with those reported by Auvinet & Rodríguez-Rebolledo (2017), they also demonstrate that the depth of such level depends significantly on the initial pile load conditions. The differences between piles in the magnitude of the axial loads is related to the corresponding influence area, e.g., the influence area of the corner pile is considerably larger than other piles leading to higher values of negative skin friction. Also, Lee (1993) stated that negative friction at an individual pile in the group is smaller than in an isolated pile due to the interaction effects.

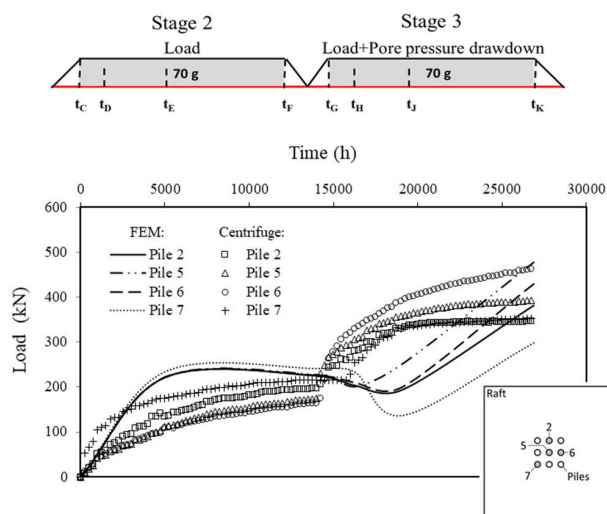


Figure 18. Load versus time curves obtained at the top of the instrumented piles 2, 5, 6 and 7 by centrifuge and FEM models, after adjustment.

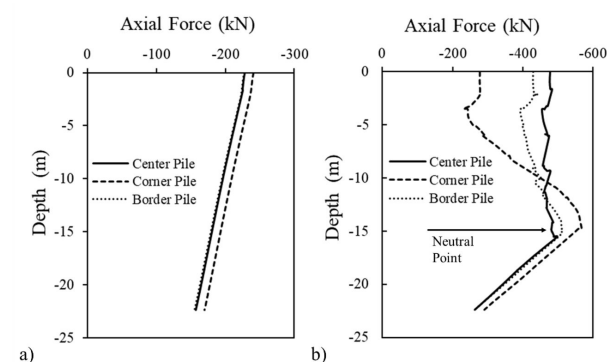


Figure 19. Axial forces developed along the piles with different positions in the piled raft (border, corner and center), for: (a) Phase 2; and (b) Phase 6.

The obtained results show the importance of considering the negative skin friction on the pile design, the maximum axial load transmitted by the piles due to the structural service load is approximately 240 kN, whereas, when porewater pressure drawdown develops, the axial load increases to 560 kN, 2.3 times higher.

4. Conclusions

In this work a 3D numerical model based on the Finite Element Method (FEM) capable of simulating the complex behavior of a piled raft system founded in soft soils undergoing regional subsidence was developed and validated by the results obtained by a geotechnical centrifuge model. This model allowed to identify the most sensitive parameters for this type of simulation, to define the types and stages of analysis that had the best fit to the physical model, and to obtain additional results to those measured in the physical model as the magnitude of the developed negative skin friction.

For the simulation of the soft soil behavior (kaolin) an advanced isotropic hardening double surface plasticity model (Hardening Soil Model, HSM) implemented in Plaxis software were used. The parameters for the HSM were obtained from oedometer and drained consolidated triaxial tests using the methodology proposed by Surarak et al. (2012) and Rodríguez-Rebolledo et al. (2019). The obtained parameters were satisfactorily calibrated and adjusted using the Soil Test tool from the Plaxis software.

Pile shaft and base resistance for long term behavior were obtained from a pile load test carried out in a centrifuge model, as they were also needed as input parameters for the chosen numerical model.

The developed numerical model reproduced satisfactorily soil and foundation consolidation displacements due, not only by the structural service load but also by the pore pressure drawdown (regional subsidence). For service load the maximum settlements reached up to 6 cm in the raft region. At the end of pore pressure drawdown, the maximum settlement was approximately 50 cm (8 times bigger). These comparative results do evidence the distinct phenomena and resulting engineering behavior that take place on a typical system founded in this type of environment.

For load distribution on piles and raft, the model reproduces with good agreement the foundation behavior only for the structural service load, for pore pressure drawdown some adjustments on the shaft and base resistance of the embedded piles elements had to be done.

For service loads differences between FEM and centrifuge models from 12 to 38% were obtained, while for pore pressure drawdown from -77 to -169%. Centrifuge model shows that from one stage to the other the load transmitted by piles increases (from 13% to 26%) while load transmitted by raft decreases (from 87 to 74%). As explained by Rodríguez-Rincón et al. (2018) this is because, when pore pressure drawdown occurs, the soil continues to settle, a movement that is not accompanied by the raft, generating an apparent emersion process, and hence, a reduction of contact between the soil and the raft. This phenomenon was not developing in the FEM model because the considered skin resistance of the piles was not enough to allow the generation of the negative skin friction necessary for this. The generated pore

pressure drawdown produces an increment in effective stresses throughout the compressible soil, leading to an increase in shear resistance. The FEM results show that the embedded pile element does not consider the increase of the shear resistance parameters related to skin friction that happen when the soil is subjected to a consolidation process. To approximately match the models results (variations in the piles loads from -4 to 21%), it was necessary to adjust the base and axial skin resistance of the embedded piles elements in about 3.5 times, demonstrating the limitation in the use of this type of elements for the simulation of this kind of problems. To avoid this problem, two solutions were proposed:

- 1) determine the long-term base and skin resistance of the embedded piles using previously a simple 2D FEM model (axisymmetric), through the simulation of a load test of a single pile in a medium previously subjected to pore pressures drawdown;
- 2) use of volume elements for problems with a relatively small number of piles, the use of this type of elements can lead to exceptionally large finite element meshes and therefore high or even irrational computational costs (time and memory).

The model evidences the development of negative skin friction in the center, border and corner piles, being higher in the corner and lower in the center one. As excess pore pressure dissipates, the neutral level of the piles stabilizes at a depth between 15 to 16 m. These results agree with those reported by Auvinet & Rodríguez-Rebolledo (2017), they also demonstrate that the depth of such level depends significantly on the initial pile load conditions. The differences between piles in the magnitude of the axial loads is related to the corresponding influence area, e.g., the influence area of the corner pile is considerably larger than other piles leading to higher values of negative skin friction.

It is finally concluded that a simulation model for piled raft foundation systems founded on consolidation soft strata, via loading or porewater pressure drawdown, is feasible with a quite reasonable approximation of the field behavior/site conditions. This will be extremely useful for future design scenarios via parametric analysis of this same system, thus aiming to optimize the performance of this type of foundation structure when undergoing a regional subsidence phenomenon.

Acknowledgements

The research of the first author is possible through a scholarship provided by the Brazilian sponsorship organization named Conselho Nacional de Desenvolvimento Científico e Tecnológico - Brazil (CNPq), which is most appreciated. The authors also want to acknowledge the Universidad de Los Andes - Colombia for their support for the development of the centrifuge modeling, and Prof. Renato P. Cunha of the University of Brasilia for the critical comments, and diligent support provided throughout the development of the numerical stage of this research.

Declaration of interest

The Authors declares that there is no conflict of interest that could inappropriately bias the work presented.

Author's contributions

Andrea J. Alarcón Posse: conceptualization, methodology, investigation, validation, writing - original draft. Juan F. Rodríguez Rebolledo: supervision, conceptualization, methodology. Julián A. Buriticá García: investigation. Bernardo Caicedo Hormaza: resources. Edgar Rodríguez-Rincón: resources.

References

- Alnuaim, A.M., El Naggar, H., & El Naggar, M.H. (2017). Evaluation of piled raft performance using a verified 3D nonlinear numerical model. *Geotechnical and Geological Engineering*, 35(4), 1831-1845. <http://dx.doi.org/10.1007/s10706-017-0212-1>.
- Alnuaim, A.M., El Naggar, M.H., & El Naggar, H. (2018). Performance of micropiled rafts in clay: numerical investigation. *Computers and Geotechnics*, 99, 42-54. <http://dx.doi.org/10.1016/j.compgeo.2018.02.020>.
- Auvinet, G., & Rodriguez-Rebolledo, J. (2017). Criteria for the design of friction piles subjected to negative skin friction and transient loads. *Ingeniería, Investigación y Tecnología*, 18, 279-292. <http://dx.doi.org/10.22201/ifi.25940732e.2017.18n3.025>.
- Bajad, S.P., & Sahu, R.B. (2008). An experimental study on the behaviour of vertically loaded piled raft on soft clay. In *Proceedings of the 12th International Conference of International Association for Computer Methods and Advances in Geomechanics*, Goa, India.
- Banerjee, S., Joy, M., & Sarkar, D. (2016). Parametric study and centrifuge-test verification for amplification and bending moment of clay-pile system subject to earthquakes. *Geotechnical and Geological Engineering*, 34(6), 1899-1908. <http://dx.doi.org/10.1007/s10706-016-9999-4>.
- Brinkgreve, R. B. J., Kumarswamy, S. & Swolfs, W. M. (2018). *Reference manual and material models manual PLAXIS*. The Netherlands.
- Cheng, S., Zhang, G., Zheng, R.H., & Sun, Z.Y. (2011). Centrifuge modeling of response of bridge due to exploiting groundwater. *Yantu Lixue*, 32(6), 1781-1786.
- Cho, J., Lee, J.H., Jeong, S., & Lee, J. (2012). The settlement behavior of piled raft in clay soils. *Ocean Engineering*, 53, 153-163. <http://dx.doi.org/10.1016/j.oceaneng.2012.06.003>.
- Cui, C., Luan, M., & Li, M. (2010a). A study on time-effects of piled raft system by using computational methods. In *Proceedings of the GeoShanghai International Conference 2010* (pp. 42-51), Shanghai, China.
- Cui, Z.-D., Tang, Y.-Q., & Yan, X.-X. (2010b). Centrifuge modeling of land subsidence caused by the high-rise building group in the soft soil area. *Environmental Earth Sciences*, 59(8), 1819-1826. <http://dx.doi.org/10.1007/s12665-009-0163-9>.
- El-Mossallamy, Y. (2008). Modeling the behaviour of piled raft applying Plaxis 3D Foundation Version 2. *Plaxis Bulletin*, (23), 1-4.
- Goh, S.H., & Zhang, L. (2017). Estimation of peak acceleration and bending moment for pile-raft systems embedded in soft clay subjected to far-field seismic excitation. *Journal of Geotechnical and Geoenvironmental Engineering*, 143(11), 04017082. [http://dx.doi.org/10.1061/\(ASCE\)GT.1943-5606.0001779](http://dx.doi.org/10.1061/(ASCE)GT.1943-5606.0001779).
- Horikoshi, K., & Randolph, M.F. (1996). Centrifuge modelling of piled raft foundations on clay. *Geotechnique*, 46(4), 741-752. <http://dx.doi.org/10.1680/geot.1996.46.4.741>.
- Khanmohammadi, M., & Fakharian, K. (2018). Evaluation of performance of piled-raft foundations on soft clay: a case study. *Geomechanics and Engineering*, 14(1), 43-50. <http://dx.doi.org/10.12989/gae.2018.14.1.043>.
- Lee, C.Y. (1993). Pile groups under negative skin friction. *Journal of Geotechnical Engineering*, 119(10), 1587-1600.
- Lee, J., Kim, Y., & Jeong, S. (2010). Three-dimensional analysis of bearing behavior of piled raft on soft clay. *Computers and Geotechnics*, 37(1-2), 103-114. <http://dx.doi.org/10.1016/j.compgeo.2009.07.009>.
- Luo, R., Yang, M., & Li, W. (2018). Normalized settlement of piled raft in homogeneous clay. *Computers and Geotechnics*, 103, 165-178. <http://dx.doi.org/10.1016/j.compgeo.2018.07.023>.
- Mali, S., & Singh, B. (2018). Behavior of large piled-raft foundation on clay soil. *Ocean Engineering*, 149, 205-216. <http://dx.doi.org/10.1016/j.oceaneng.2017.12.029>.
- Ng, C.W.W. (2014). The state-of-the-art centrifuge modelling of geotechnical problems at HKUST. *Journal of Zhejiang University. Science A*, 15(1), 1-21. <http://dx.doi.org/10.1631/jzus.A1300217>.
- Nordal, S. (1999). Present of PLAXIS. In R.B.J. Brinkgreve (Ed.), *Beyond 2000 in Computational Geotechnics: ten years of PLAXIS International* (pp. 45-54). London: Routledge.
- Oliveira, B. (2018). *Avaliação do atrito negativo em grupos de estacas assentes em solos moles* [Master's dissertation]. Universidade de Brasília.
- Rodríguez Rebolledo, J.F., Auvinet-Guichard, G.Y., & Martínez-Carvajal, H.E. (2015). Settlement analysis of friction piles in consolidating soft soils. *Dyna*, 82(192), 211-220. <http://dx.doi.org/10.15446/dyna.v82n192.47752>.
- Rodríguez-Rebolledo, J.F. (2011). *Modeling behavior of piles and inclusions under regional consolidation in the lake area of Mexico City* (244 p.). Mexico: National Autonomous University of Mexico. (In Spanish).
- Rodríguez-Rebolledo, J.F., León, R.F.P., & Camapum de Carvalho, J. (2019). Obtaining the mechanical parameters for the hardening soil model of tropical soils in the city of Brasília. *Soils and Rocks*, 42(1), 61-74. <http://dx.doi.org/10.28927/SR.421061>.

- Rodríguez-Rincón, E. (2016). *Experimental analysis of piled raft systems in consolidating soft soils* (261 p.). Brasília: Universidade de Brasília. (In Portuguese).
- Rodríguez-Rincón, E., Cunha, R.P., & Caicedo Hormaza, B. (2020). Analysis of settlements in piled raft systems founded in soft soil under consolidation process. *Canadian Geotechnical Journal*, 57(4), 537-548. <http://dx.doi.org/10.1139/cgj-2018-0702>.
- Rodríguez-Rincón, E., Cunha, R.P., & Caicedo, B. (2018). Behaviour of piled raft foundation systems in soft soil with consolidation process. In *Proceedings 9th Int. Conf. on Physical Modelling in Geotechnics*, London.
- Roy, S., & Chattopadhyay, B. C. (2011). Piled-Raft foundation behaviour on consolidating soft soil. In *Proceedings of the International Conference on Structural Engineering Construction and Management*, Kandy.
- Schanz, T., Vermeer, P. A., & Bonnier, P. G. (1999). The hardening soil model: formulation and verification. In R.B.J. Brinkgreve (Ed.), *Beyond 2000 in Computational Geotechnics: ten years of PLAXIS International* (pp. 281-296). London: Routledge.
- Sinha, A., & Hanna, A.M. (2017). 3D numerical model for piled raft foundation. *International Journal of Geomechanics*, 17(2), 04016055. [http://dx.doi.org/10.1061/\(ASCE\)GM.1943-5622.0000674](http://dx.doi.org/10.1061/(ASCE)GM.1943-5622.0000674).
- Sun, Z., Zhang, G., Zhang, J., Li, G., & Zheng, R. (2008). Centrifuge modeling of ground settlement due to groundwater pumping. *China Civil Engineering Journal*, 41(4), 67-72.
- Surarak, C., Likitlersuang, S., Wanatowski, D., Balasubramaniam, A., Oh, E., & Guan, H. (2012). Stiffness and strength parameters for hardening soil model of soft and stiff Bangkok clays. *Soil and Foundation*, 52(4), 682-697. <http://dx.doi.org/10.1016/j.sandf.2012.07.009>.
- Tang, Y.Q., Ren, X., Chen, B., Song, S., Wang, J.X., & Yang, P. (2012). Study on land subsidence under different plot ratios through centrifuge model test in soft-soil territory. *Environmental Earth Sciences*, 66(7), 1809-1816. <http://dx.doi.org/10.1007/s12665-011-1406-0>.
- Thaher, M., & Jessberger, H. (1991). Investigation of the behaviour of pile-raft foundation by centrifuge modelling. In *Proceedings of the 10th European Conference on Soil Mechanics and Foundation Engineering* (Vol. 2, pp. 597-603), Firenze, Itália.
- van Tran, T., Kimura, M., & Boonyatee, T. (2012b). 3D FE analysis of effect of ground subsidence and piled spacing on ultimate bearing capacity of piled raft and axial force of piles in piled raft. *Open Journal of Civil Engineering*, 2(4), 206-213. <http://dx.doi.org/10.4236/ojce.2012.24027>.
- van Tran, T., Teramoto, S., Kimura, M., Boonyatee, T., & Vinh, L.B. (2012a). Effect of ground subsidence on load sharing and settlement of raft and piled raft foundations. *Stress*, 1(3), 120-127.
- Wang, J., Huang, T., & Sui, D. (2013). A case study on stratified settlement and rebound characteristics due to Dewatering in Shanghai Subway Station. *The Scientific World Journal*, 2013, 213070. <http://dx.doi.org/10.1155/2013/213070>.
- Watcharasawe, K., Kitiyodom, P., & Jongradist, P. (2015). Numerical analyses of piled raft foundation in soft soil using 3D-FEM. *Geotechnical Engineering*, 46(1), 109-116.
- Zhang, L., & Liu, H. (2017). Seismic response of clay-pile-raft-superstructure systems subjected to far-field ground motions. *Soil Dynamics and Earthquake Engineering*, 101, 209-224. <http://dx.doi.org/10.1016/j.soildyn.2017.08.004>.
- Zhang, L., Goh, S.H., & Liu, H. (2017b). Seismic response of pile-raft-clay system subjected to a long-duration earthquake: centrifuge test and finite element analysis. *Soil Dynamics and Earthquake Engineering*, 92, 488-502. <http://dx.doi.org/10.1016/j.soildyn.2016.10.018>.
- Zhang, L., Goh, S.H., & Yi, J. (2017a). A centrifuge study of the seismic response of pile-raft systems embedded in soft clay. *Geotechnique*, 67(6), 479-490. <http://dx.doi.org/10.1680/jgeot.15.P.099>.

List of symbols

α is an auxiliary parameter of the model
 β auxiliary parameter of the model related to the reference tangent stiffness modulus for oedometric loading
 γ_p plastic shear strain
 φ' Internal friction angle
 σ'_3 confining stress in the triaxial test
 ψ dilatancy angle
 c' Cohesion
 ε axial strain
 ε_I vertical strain
 ε_I^p plastic axial strain
 ε_v^{pc} volumetric plastic strains in isotropic compression
 ε_v^p plastic volumetric strain
 E_i initial stiffness
 E_{oed} axial stress-dependent stiffness modulus for primary oedometric loading
 E_{s0} is the confining stress-dependent stiffness modulus for the primary load
 E_{ur} stress-dependent stiffness modulus for unloading and reloading stress
 E_{s0}^{ref} reference secant stiffness modulus for the drained triaxial test
 E_{oed}^{ref} reference tangent stiffness modulus for oedometric loading
 E_{ur}^{ref} reference stiffness modulus for unloading and reloading conditions
 f^c cap compression hardening yield function
 f_s shear hardening yield function
 K_o^{nc} coefficient of earth pressure at rest (NC state)
 K_o coefficient of earth pressure at rest
 m Exponential power
 OCR Over Consolidation Ratio
 p is the isotropic stress
 p_p is the pre-consolidation isotropic stress
 p_{ref} Stress of reference
 q deviatoric stress
 q_a asymptote of the shear strength
 q_f ultimate deviatoric stress at failure
 \bar{q} is the special stress measurement for deviatoric stresses
 R_f failure ratio
 ν_{ur} Unloading/reloading Poisson's Ratio